

Iron clusters supported in a zeolite matrix: Comparison of different magnetic characterizations

F. J. Lázaro and J. L. García

Instituto de Ciencia de Materiales de Aragón (Universidad de Zaragoza-Consejo Superior de Investigaciones Científicas), 50015 Zaragoza, Spain

V. Schünemann and Ch. Butzlaff

Institut für Physik, Medizinische Universität, 2400 Lübeck, Germany

A. Larrea

Instituto de Ciencia de Materiales de Aragón (Universidad de Zaragoza-Consejo Superior de Investigaciones Científicas), 50015 Zaragoza, Spain

M. A. Załuska-Kotur

Institute of Physics, Polish Academy of Sciences, 02-668 Warszawa, Poland

(Received 24 March 1995; revised manuscript received 11 January 1996)

Metallic iron clusters dilutely supported in zeolite NaX have been studied by magnetization, ac susceptibility, and transmission electron microscopy. Their behavior is superparamagnetic at high temperatures with negligible intercluster interactions and the cluster magnetic moments become blocked at low temperatures. From the ac susceptibility data, at frequencies between 1 Hz and 1 kHz in the temperature range 1.8–300 K, the distribution of activation energies has been determined. The results have been used to check a previously proposed scaling of the ac susceptibility and justify the use of the Arrhenius law for these systems. Although the obtained information is limited by the temperature and frequency window of the experiment, the quantitative analysis of the ac susceptibility provides, with respect to the magnetization data, additional information about the actual distribution of cluster sizes and it is a valuable tool to avoid misinterpretations about the interaction effects. [S0163-1829(96)08619-5]

I. INTRODUCTION

Small magnetic particle research generally deals with single domain entities that, according to their size, can be classified into three groups: (a) those with sizes around tenths of micrometers, as those typically used for magnetic recording,¹ (b) the nanometric ones, approximately between 500 and 50 Å, that find application for example in ferrofluids,² and (c) the still smaller ones, whose properties clearly start to deviate from those of the bulk, which could better be called clusters.³ Particles of the first group are relatively large, hence, at room temperature, they keep a stable magnetization while the second and the third types are generally superparamagnetic.

Among the many research lines in this field one would mention the challenge of achieving a narrow particle size distribution, the characterization of how properties of the particle assembly start to deviate from the corresponding properties of the bulk material as the particle size decreases, and the study of the influence of particle inhomogeneities. There are very beautiful examples of large particles with remarkably narrow size and shape distributions,⁴ this quality is, however, more difficult to attain on the nanometric scale. The properties of the extremely fine particles (those on the mesoscopic scale) are generally studied in experiments on free clusters.⁵ Alternatively, magnetic data on supported clusters correspond to the so-called cluster compounds.⁶

Nanometric particles have been studied extensively as the main constituents of magnetic fluids⁷ or located into amorphous matrices such as silica⁸ or epoxy resins.⁹ Nevertheless, from the point of view of their physical properties, little ef-

fort has gone into using crystalline hosts until now. In this sense, zeolites, which are well known as very efficient aluminosilicate molecular sieves¹⁰ and meet the requirement of crystallinity, may constitute a promising type of matrix in order to obtain materials with novel properties. This idea is supported by some recent discoveries, such as the observation of ferromagnetism in potassium when it fills the cavities of zeolite LTA.¹¹

Ferrofluids are very useful for fundamental studies on small particles because, by dilution, many samples can be prepared with a continuous variation of the dipolar interaction but keeping the same size distribution. Zeolites might constitute, however, a suggestive alternative. Their cavities have a well-defined geometry and they are regularly arranged in space, therefore particle dimensions would theoretically be constrained, rather independently of the concentration of particles. This is in fact one of the aims of the present study.

In this work an extensive magnetic characterization of iron clusters in zeolite NaX has been performed. On the basis of their magnetic properties, a combined discussion of several granulometric methods, with a particular emphasis on the application of techniques that involve magnetic relaxation, is presented.

II. SAMPLE PREPARATION AND EXPERIMENTAL METHODS

The samples have been prepared by thermal decomposition of Fe(CO)₅ in zeolite NaX. NaX is a Faujasite-type zeolite and it contains cavities 13 Å in diameter connected by pores of 8 Å. The structure is cubic with eight supercages per

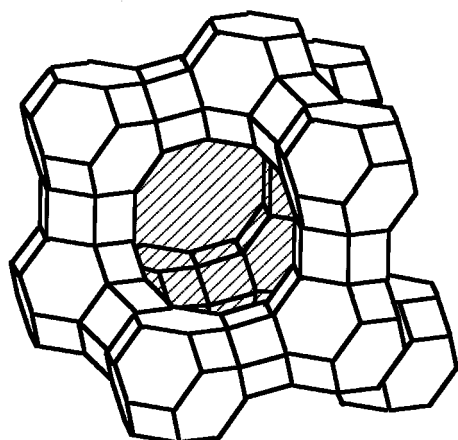


FIG. 1. Schematic view of the Faujasite structure. The shaded area indicates the location of the 13-Å-diam supercage, with tetragonal symmetry, as it is viewed through the pores of 8 Å. The vertices of polyhedra correspond to silicon or aluminum positions. The truncated octahedra are the so-called sodalite units.

unit cell (lattice parameter, 24.67 Å; density, 1.91 g/cm³) (see Fig. 1).¹⁰

After dehydration at 673 K the iron pentacarbonyl is adsorbed at low temperature (77 K), it is further decomposed by heating up to 453 K under static vacuum and it is heated up to 823 K under high vacuum.

The iron loaded zeolite powder is synthesized in a large glass container. The synthesized powder was then moved to one end of the glass container and this part of the container was further sealed resulting in a small glass capsule. Beforehand this capsule is filled with helium gas in order to improve the thermal contact during the measurements and to keep the iron free from oxidation. It should be taken into account that, because of this encapsulation procedure, there exist strong difficulties in determining the weight of the samples, therefore the information obtained from the magnetic measurements will be limited slightly, as will be explained later.

Previous Mössbauer experiments on the same samples indicated that at least 90% of the iron is in the metallic state.¹² The rest is present as Fe(II) but this fact is not relevant to get the conclusions of this paper.

Three samples have been studied by magnetic measurements. A fourth one, exposed to air and allowed to oxidize, has been used for the transmission electron microscopy (TEM) analysis (see Table I). Sample Z1B was prepared in the same way as sample Z1S but, because of being enclosed in a smaller glass capsule, it was heated when applying the

TABLE I. Description of the samples studied. The volumetric fraction ϵ is defined as the fraction of the total volume occupied by magnetic material, assuming all the iron is present as α -Fe.

Sample	wt. % Fe	ϵ	Color
Z1S	4	0.0064	Grey
Z1B	4	0.0064	Grey
Z2	2	0.0032	Grey
Z3	same as Z1S but oxidized in air		Light brown

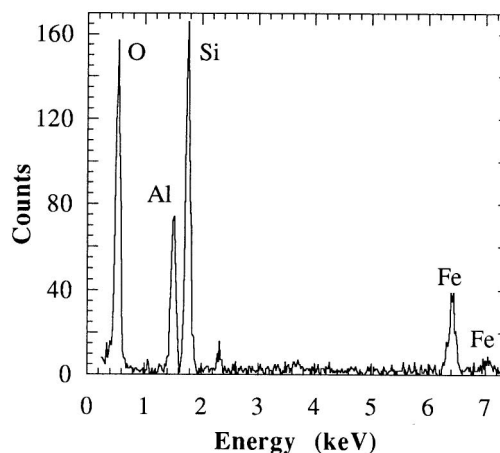
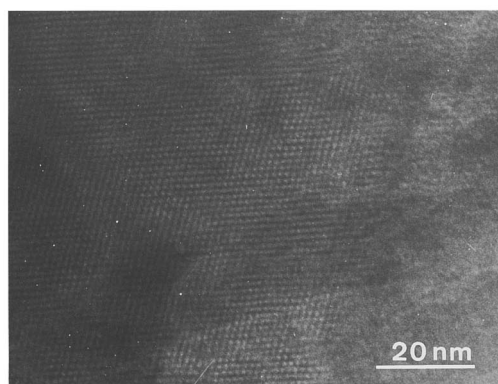


FIG. 2. Transmission electron microscopy (TEM) results. (a) High-resolution micrograph of sample Z3 showing the periodic arrangement of the supercages. (b) X-ray energy dispersive spectrum corresponding to the zone shown in (a).

flame during the sealing process. As will be shown later, the magnetic behavior was altered for this reason.

The magnetization as well as the ac susceptibility have been measured using a superconducting quantum interference device apparatus (Quantum Design). The TEM experiments have been performed in a JEOL 2000 FX II microscope, equipped with an Oxford/LINK energy dispersive spectrometry (EDS) analytical system.

III. TRANSMISSION ELECTRON MICROSCOPY

The possible existence of particles much larger than the zeolite supercages has been investigated by TEM. In Fig. 2(a) a representative region of the zeolite is shown. The picture is a high-resolution electron micrograph (HREM) of the iron loaded zeolite after exposure to air and further oxidation (sample Z3). The previously existing iron particles have partly been transformed to some iron oxide but they should still remain in the zeolite. Therefore, if there is no trace of large particles in Z3, the corresponding nonoxidized sample Z1S must be free of them too.

In the TEM picture, it is not possible to distinguish any other structure than the regular arrangement of supercages. It is known that the raw HREM image, if no further image treatment is performed,¹³ is not sufficient to assess whether the cages are occupied or not. In our case the spatial resolution of the microscope (2.8 Å) together with the higher

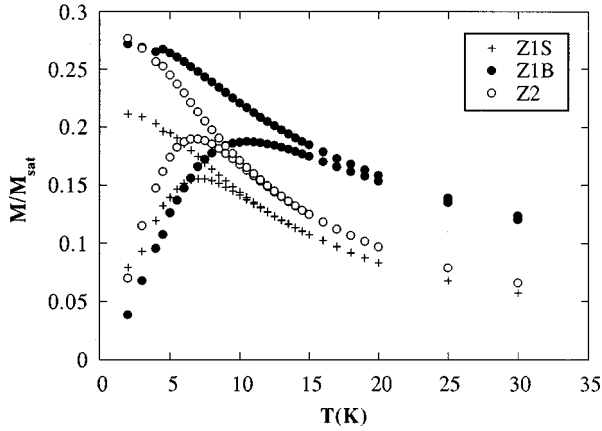


FIG. 3. Temperature dependence of the magnetization of samples Z1S, Z1B, and Z2, using an external field of 10 mT. Field-cooled FC (upper curves), zero-field-cooled ZFC (lower curves).

atomic number of Fe compared to Si, Al, and other elements in the zeolite make unlikely the existence of iron clusters greater than two or three supercages because otherwise they will be visible in the HREM image.

The TEM characterization has been completed by performing a EDS microanalysis on the same area corresponding to the HREM image. As expected, the spectrum [Fig. 2(b)] shows the Fe $K\alpha$ and Fe $K\beta$ x-ray fluorescence lines clearly indicating the presence of iron. The same microanalysis was performed on a specimen of unloaded zeolite NaX resulting in an identical spectrum except for the lack of the peaks due to iron.

One should also keep in mind that the iron atoms did not belong to the zeolite framework, instead they have been *condensed inside the cavities at the stage of decomposition of Fe(CO)₅*. Therefore we should discard any eventual contribution of in-framework iron to the EDS spectrum.

IV. MAGNETIC CHARACTERIZATION

A. Magnetization versus temperature

The magnetization of the three iron loaded samples has been studied as a function of temperature with a dc applied field of 10 mT (see Fig. 3). In the plot, the magnetization is shown relative to the saturation magnetization M_{sat} . This one has been calculated for each sample by making an approach to saturation of the $M(H)$ data (see next section). Below a given temperature T_d , the field-cooled (FC) and the zero-field-cooled (ZFC) curves do not superimpose due to slow magnetic relaxation of large particles. The temperature T_m , where the maximum of the ZFC curve takes place, is very similar for samples Z1S and Z2, and the same happens for T_d . This can be interpreted as follows. In spite of having different iron contents, samples Z1S and Z2 have a very similar distribution of particle sizes while sample Z1B contains larger particles. It may be caused by the mentioned heating of sample Z1B, in fact the growth of clusters upon thermal treatment is a well-known effect in zeolites.^{14,15}

One should notice in Fig. 3 that, in the case of sample Z1B, the measured FC and ZFC magnetization only coincide at the highest temperature of the experiment. This means that the so defined T_d must be equal to or greater than 30 K,

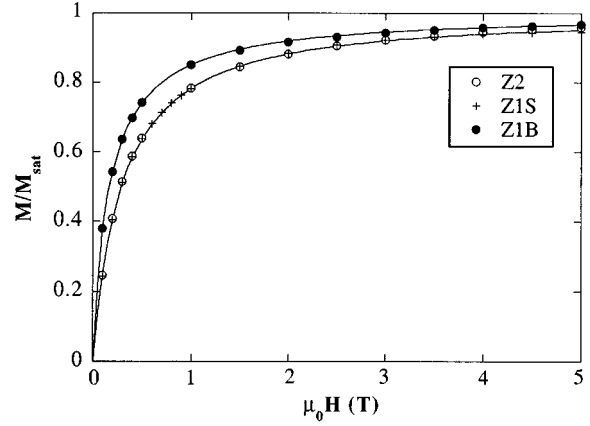


FIG. 4. Magnetization curves at 77 K of samples Z1S, Z1B, and Z2. The fits of the experimental data in terms log-normal distributions are represented as continuous lines.

indicating that Z1B contains a small amount of large particles already blocked at that temperature. For decreasing temperature, below T_m , the FC magnetization still increases in all the cases, indicating that there are still small unblocked particles that behave independently of the rest of the particles, that is, there is no cooperative freezing of the magnetic moments but an overall single-particle superparamagnetic blocking.

B. Magnetization versus applied field

The field dependence of the magnetization has been measured at 77 K under applied fields up to 5 T. The results are shown in Fig. 4. The magnetization is shown relative to the saturation value M_{sat} of each sample.

Samples Z1S and Z2, as will be concluded from the ac susceptibility analysis (see Sec. IV C), are at 77 K in a full superparamagnetic state while sample Z1B possesses a small fraction of particles, generated during the thermal treatment, which are large enough to undergo blocking around that temperature range.

The magnetization curves $M(H)$ are often used to determine the particle size distribution. One generally considers an assembly of noninteracting particles such that $M(H)$ follows a Langevin law for each particle size. At low temperatures the single-particle anisotropy leads to deviations of $M(H)$ from the pure Langevin behavior,¹⁶ which limits the use of $M(H)$ data to high temperatures. It is very common¹⁷ to use a log-normal distribution

$$f(y) = \frac{1}{y\sigma\sqrt{2\pi}} \exp\left[-\frac{(\ln y)^2}{2\sigma^2}\right], \quad (1)$$

where $y = D/D_v$, D is the particle diameter, D_v the median value of the distribution, and $f(y)dy$ is the fraction of the total volume occupied by particles with reduced diameters between y and $y + dy$. This functional form can be justified in particulate systems such as ferrofluids where the actual distribution is with a good approximation log-normal. Nevertheless, it should be noted here that, in our case, the use of such a distribution function must be considered as a first approximation, given the well defined size of the matrix cavities.

The parameters characterizing the log-normal distributions are shown in Table II. It is known that on the nanometric range the spontaneous magnetization M_s depends on the particle size.¹⁸ However, in order to obtain the cluster sizes, we have used in our case the approximation $M_s(\text{clusters}) \approx M_s(\text{bulk } \alpha\text{-iron})$.

As can be seen, samples Z1S and Z2 exhibit a very similar size distribution while sample Z1B contains larger particles.

C. ac susceptibility versus temperature and frequency

The temperature dependence of the ac susceptibility is shown in Fig. 5. The ac exciting field has been 0.11 mT and the three frequencies used 1, 120, and 1000 Hz. The in-phase component, in all the cases, presents a high-temperature tail corresponding to superparamagnetic behavior and a frequency-dependent peak, at a temperature T_B , due to relaxation, as it happens for small particle systems.⁸ A sizable out-of-phase component is also observed at those temperatures where there is a departure from superparamagnetism, due to magnetic blocking. Susceptibilities of samples Z1S and Z2 look very similar, with the relaxation anomaly at the same temperature. On the contrary, Z1B shows a higher T_B , in agreement to the $M(T)$ results.

In paramagnetic and superparamagnetic systems, some information is often obtained by inspection of the $1/\chi'$ versus T line. When this line, assumed straight, presents a nonzero intercept with the temperature axis, one generally speaks about the existence of interactions between the magnetic moments. However, for fine particle systems, this way of reasoning must be accompanied by a great precaution because several effects, and not only interactions, can be involved simultaneously. A thorough discussion of this problem, with particular emphasis on the dc case, has already been given.¹⁹

Figure 6 shows the temperature dependence of the reciprocal of the in-phase susceptibility. Samples Z1S and Z2 follow a Curie-Weiss law with intercepts with the temperature axis never exceeding about 2 K. These data are represented in arbitrary units, independent for each sample, due to the problems in the mass determination mentioned in Sec. II.

At the highest temperatures $1/\chi'$ is bended upwards in Z2. The high-temperature susceptibility, and particularly its reciprocal value, is affected by the $M_s(T)$ dependence of the magnetic material constituting the clusters. It has been observed that, for very fine particles, this dependence differs from that of bulk iron and is size dependent.¹⁸ This effect should necessarily be considered here, but its rigorous correction in the present case is not possible, given the existence of a distribution of cluster sizes and the lack of reference experimental data for each particle size. Definitely, for these extremely small particles, we do not find it adequate to correct the data by using the spontaneous magnetization $M_s(T)$ of bulk iron.

In order to get information about any an additional contribution due to the zeolite matrix, the susceptibility of unloaded zeolite NaX has also been measured (data not shown here). Its mass susceptibility is positive, almost temperature independent, and of the order of $3.2 \times 10^{-3} \text{ m}^3/\text{kg}$. From a rough estimate of the masses of our samples we conclude that this contribution represents about 10 and 20% of the susceptibility at 300 K of Z1S and Z2 respectively, but only

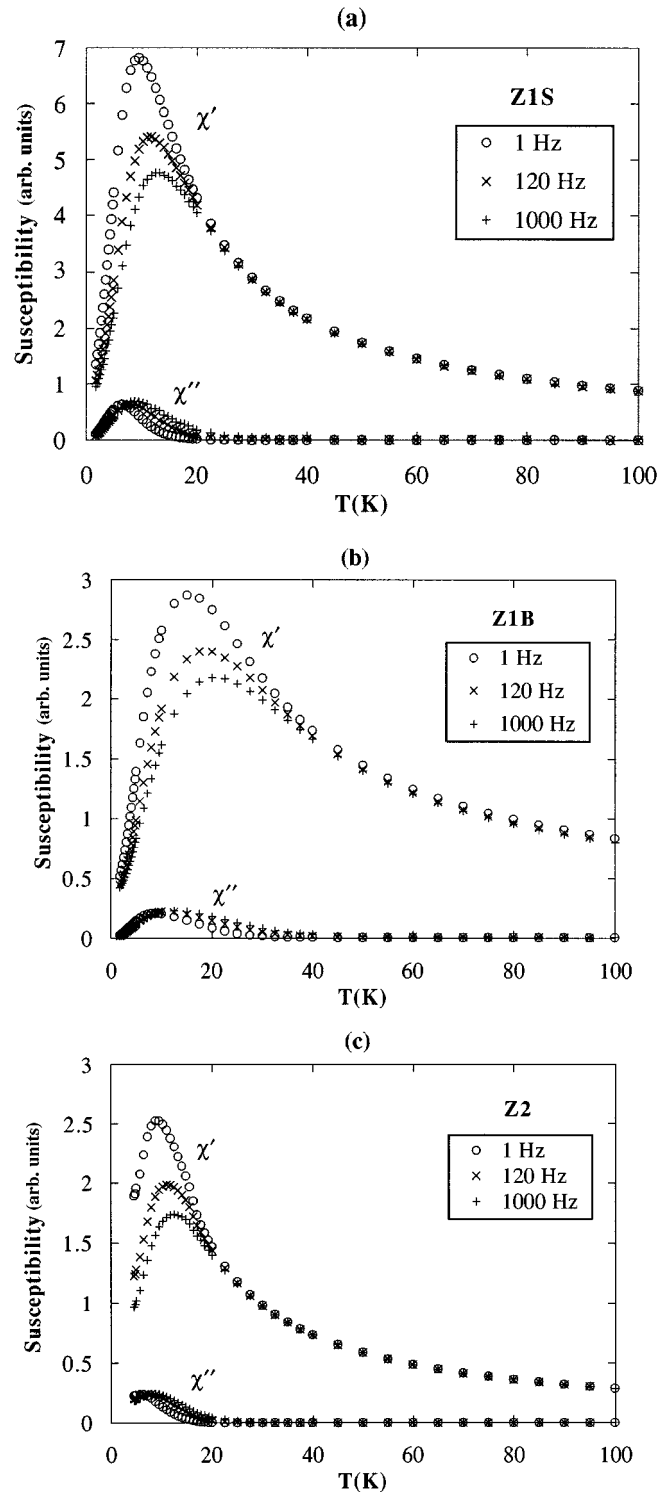


FIG. 5. Temperature dependence of the in-phase and out-of-phase components of the ac susceptibility. (a) Sample Z1S, (b) sample Z1B, and (c) sample Z2.

less than 3% in the case of Z1B. Therefore, the apparently straight $1/\chi'$ versus T line, in the case of sample Z1S, should not necessarily be understood as a pure Curie law but probably the result of cancellation of opposite effects such as the just mentioned matrix contribution and the temperature decrease of the spontaneous magnetization.

Sample Z1B shows deviations from Curie-Weiss behavior. $1/\chi$ versus T is by no means a straight line. In principle

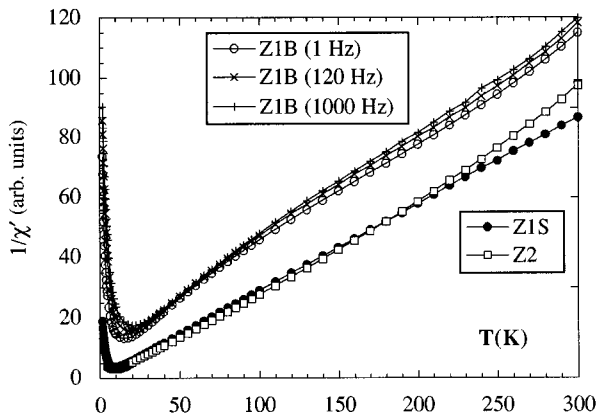


FIG. 6. Temperature dependence of the reciprocal of the in-phase susceptibility. Data for sample Z1B include the three frequencies studied. Data for samples Z1S and Z2 have only been shown at 1 Hz for clarity. The systematic frequency dependence observed above 100 K for sample Z1B does not occur at all in samples Z1S and Z2.

we could think about the existence of interactions between particles or, alternatively, about the presence of a small fraction of large particles undergoing blocking around 200 K. In general, at sufficiently high temperatures interparticle interactions are not expected to give rise to new relaxation phenomena, while the blocking of large particles would indeed be detected using a dynamic technique. To discern between these two possibilities, the ac susceptibility has been measured at different frequencies. The behavior of Z1B is substantially different from that of Z1S and Z2. In the case of Z1B, and above 100 K, χ' decreases for increasing frequency: on the contrary, no dependence at all is observed in the case of Z1S and Z2. Furthermore, the out-of-phase susceptibility of Z1B is positive in the whole temperature range while for the other two samples χ'' is zero, within the experimental accuracy, above approximately 50 K.

V. DISCUSSION

The experimental results on $M(T)$ and $\chi(T)$ indicate magnetic relaxation in the three iron loaded samples at the lowest temperatures. The results resemble those previously published for other assemblies of magnetic particles. The rounded peaks in $M_{ZFC}(T)$ as well as in $\chi'(T)$ are due to the progressive magnetic blocking of the clusters.

The importance of dipolar interaction depends on the amount of magnetic material in the sample. In our case, the low magnetic volumetric factor ϵ suggests that this effect must be negligible compared to the single-particle magnetic blocking. This can be explained as follows. Let us define a characteristic temperature $T_{\text{dip}} = \mu^2 / (k_B a^3)$ where $\mu = M_s V$ (M_s is the spontaneous magnetization of α -Fe and V is the volume of the NaX supercage) and a represents the lattice parameter of a hypothetical simple cubic lattice of the same number of lattice points per unit volume as clusters in the sample. After this, one gets $T_{\text{dip}} = 0.04$ and 0.02 K for samples Z1S and Z2 respectively, both well below their respective average blocking temperatures. Furthermore, sample Z1S has twice the iron content of Z2 but its susceptibility peak is located at the same temperature, indicating

that for those iron concentrations we are in the noninteracting regime. Within the experimental accuracy, the superimposition of the FC and ZFC curves above 15 K and the frequency independence of χ_{ac} above approximately 50 K, in the case of Z1S and Z2, suggest that all the clusters are superparamagnetic above these temperatures, that is, the $1/\chi$ versus T slope is not simultaneously affected by compensating effects, like interaction and blocking, as was shown to occur in some cases.¹⁹ Sample Z1B behaves in a different manner but, as the volumetric factors of Z1S and Z1B are the same, it can be concluded that, due to the thermal treatment, larger particles are present in Z1B. In other words, the bending of the $1/\chi(T)$ line should not be associated to interaction effects but to magnetic relaxation. This assertion is fully corroborated by the frequency dependence of the susceptibility shown in Fig. 6.

The effect of the magnetic dipolar interaction on the high-temperature susceptibility can also be roughly estimated by using a Lorentz approach. If the magnetic moments are randomly located in the material, one can use the expression $(1/\chi) = (1/\chi_m) - (N - 1/3)\rho$, where N is the sample demagnetization factor, ρ is the sample density, and χ and χ_m are the intrinsic and the measured mass susceptibility, respectively. After this, the consideration of dipolar interaction effects leads to a vertical shift of the $1/\chi$ versus T line. This shift depends on the sample shape and its maximum value, in the worst case, takes place for an infinite slab when the field is perpendicular to the slab plane. It yields an equivalent horizontal shift of around 1.4 K. This value, which should be considered as an upper bound, is very low compared to the intercept with the T -axis estimated for Z1B, therefore the dipolar interaction can be excluded from causing the anomalous behavior of this sample.

In the present case, the average effective magnetic moments cannot be calculated from the slopes of the $1/\chi'$ versus T data because of the inaccuracy in the mass determination. Nevertheless, if the magnetic relaxation observed is only due to thermally activated jumps over anisotropy energy barriers, the distribution of activation energies can be determined from the ac susceptibility. If the system is considered an assembly of noninteracting particles, the Arrhenius law $\tau = \tau_0 \exp(E/k_B T)$ holds, where τ is the single-particle relaxation time and E is the activation energy associated to the change in moment direction. The activation energy depends on geometric and magnetic particle parameters and, although the preexponential factor τ_0 introduces some uncertainty, the distribution of cluster sizes could be obtained provided one makes some additional assumptions about those dependences.

The determination of activation energies from $\chi(T)$ data is an issue handled a long time ago. Until now this problem has been treated in the fields of fine magnetic particle systems as well as in spin glasses. The source of data has sometimes been the dc susceptibility²⁰ and in others the ac susceptibility, this one treated either analytically^{21,22} or numerically.²³ Compared to the dc susceptibility, χ_{ac} has the advantage of probing the system with different measuring times; therefore it provides substantial information about the temperature dependence of the relaxation times. Let $g(E)dE$ be the fraction of the total number of particles with activation energies between E and $E + dE$. Assuming Debye-type

relaxation, the complex susceptibility can be written as

$$\chi(T, \omega) = \frac{\mu_0}{3k_B T} \int_0^\infty dE \frac{M_s^2 [V(E)]^2 g(E)}{1 + i\omega\tau}, \quad (2)$$

where the particle volume V is a function of E and where ω is the angular measuring frequency. Recently, within the research on quantum tunneling of magnetization, a method based on the scaling of the ac susceptibility data with the temperature has been proposed.²⁴ Using this method, which assumes the Arrhenius law for the temperature dependence of the relaxation times, one obtains a distribution of activation energies $n(E)$ that is proportional to the following expression:

$$n(E) \sim \frac{1}{\ln(\nu_0/\omega)} \frac{\partial}{\partial T} [T\chi'(T, \omega)], \quad (3)$$

where $\nu_0 = 1/\tau_0$ and $E = k_B T \ln(\nu_0/\omega)$. In our case, the resulting distribution function $n(E)$ has the meaning of $V^2 g(E)$ because, as a slight variation with respect to Ref. 24, we have admitted here a distribution of particle volumes. The function $n(E)$ only depends on the characteristics of the sample, hence it will not depend on the frequency used in the experiment. Therefore, if the assumed temperature dependence of the relaxation times is correct, the $n(E)$ points resulting from χ_{ac} data at different frequencies should be superimposed on a master curve.

Instead of using the function $n(E)$, it is also possible to carry out the scaling analysis by means of a function of the particle size. For this purpose we have chosen the function $f(D)$, where $f(D)dD$ stands for the volume fraction of particles with diameters between D and $D+dD$. This function is related to $n(E)$ by the expression

$$f(D) = \frac{1}{V} n(E) \frac{dE}{dD}. \quad (4)$$

With this type of representation it is possible, just in a single plot, to check the goodness of the χ_{ac} scaling and to get some information about the particle size distribution. Of course the transformation from $n(E)$ to $f(D)$ can only be made if one knows the dependence of E on D . One should bear in mind that the activation energy may not be simply proportional to the particle volume due to surface effects.²⁵ Nevertheless, as an approximation, we have considered here an activation energy for each particle $E = KV$, where K is an effective anisotropy constant. This conversion has been performed by using $K = 1.86 \times 10^5 \text{ J/m}^3$, as was previously determined by ferromagnetic resonance (FMR) measurements for the same material.^{26,27} The results are shown in Fig. 7, together with the distributions obtained from the $M(H)$ analysis.

In our case, ν_0 has been determined by fitting the peak temperatures T_B of the in-phase susceptibility to the expression

$$\ln(\omega) = \ln(\nu_0) - \frac{\alpha \bar{E}}{k_B T_B}, \quad (5)$$

giving $\nu_0 = 1.25 \times 10^{12}$, 1.35×10^{13} , and $4.56 \times 10^{12} \text{ s}^{-1}$ for Z1S, Z1B, and Z2, respectively. This formula, where α de-

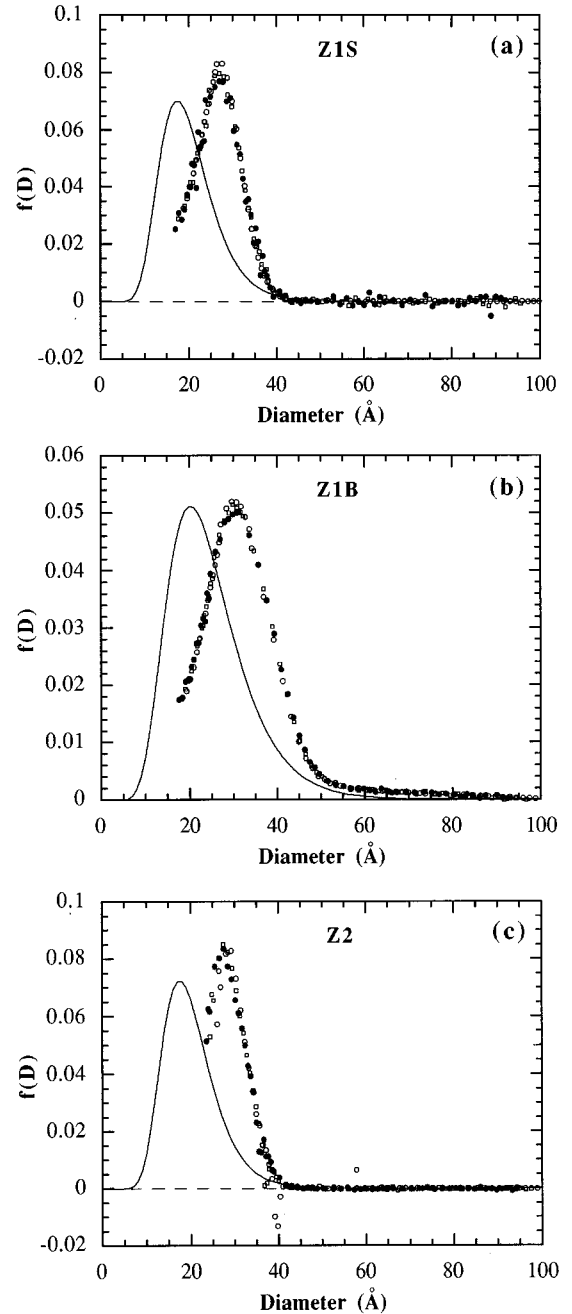


FIG. 7. Scaling plots of the ac susceptibility. (a) Sample Z1S, (b) sample Z1B and (c) sample Z2. The function shown is $f(D)$, related to $n(E)$ by expression 4. The symbols represent data obtained from $\chi'(T)$ at the following frequencies: ●, 1000 Hz; □, 120 Hz; and ○, 1 Hz. The continuous line represents the log-normal distribution obtained by analyzing the $M(H)$ data.

pends on the type of distribution and \bar{E} is the average activation energy, has been derived previously.²¹ We tried to use other methods to obtain τ_0 , such as the one proposed in Ref. 24. These other methods, which rely on numerical derivatives of the experimental data, did not improve the scaling in our case, but merely resulted in higher errors in the determination of the preexponential factor. It seems, however, that, in the general case, the quality of the ac susceptibility scaling can be very sensitive to the change of τ_0 .

Using the preexponential factors indicated above, a very good overlap of the $f(D)$ distributions resulting from χ_{ac} at

TABLE II. Parameters of the distributions of cluster sizes obtained from $M(H)$ and χ_{ac} data. D_v and σ are the parameters of the log-normal $f(y)$ distribution. Columns labeled $D_m(g)$ and $D_m(f)$ contain the diameters corresponding to the maxima of the fraction of number of particles and volume fraction distributions, respectively. Diameters are given in angstroms.

Sample	$M(H)$ analysis				χ_{ac} analysis	
	D_v	σ	$D_m(g)$	$D_m(f)$	$D_m(g)$	$D_m(f)$
Z1S	19.2	0.31	13.1	17.4	<25	27
Z1B	23.1	0.36	13.8	20.3	<25	30
Z2	19.2	0.30	13.4	17.5	<25	28

different frequencies is achieved. The size distributions of samples Z1S and Z2 are very similar and in both cases they drop to zero at approximately 40 Å [see Figs. 7(a) and 7(c)]. On the other hand, the existence in Z1B of a small fraction of large particles, with diameters up to about 90 Å, is neatly observed in this kind of plot [Fig. 7(b)].

In order to discuss the range of validity of the size analyses performed from the $M(H)$ and χ_{ac} data, we should first make the following considerations.

The distributions obtained from $M(H)$ represent in fact the distribution of magnetic moments. Therefore, it is necessary to make a transformation to particle sizes by assuming a value for M_s . This value has been taken as the spontaneous magnetization of bulk iron but, although it is the best value at hand, it may not be fully realistic in the case of very small particles.¹⁸ On the other hand, in this type of analysis, the size distribution function is forced *a priori* to be log-normal, with the risk of biasing the results.

The analysis from χ_{ac} is based on magnetic relaxation and the resulting distributions correspond to the spectrum of activation energies. As explained above, the transformation from activation energies to cluster sizes has been performed by using an average value for the anisotropy constant (that from FMR). This constant may depend on cluster size but its explicit dependence is unknown, hindering any further refinement of this analysis. Nevertheless, the virtue of this treatment resides in the *direct* obtainment of the distribution of activation energies without imposing any functional form.

Although both methods are subjected to some limitations, as has been discussed above, it is possible, however, to compare the resulting cluster sizes with the physical dimensions of the cavities and pores of the zeolite framework. The comparison can be made by using either the fraction of number of clusters $g(D)$ or the volume fraction $f(D)$ distribution functions. Table II contains the diameters D_m corresponding to the absolute maxima of the distributions obtained from $M(H)$ and from χ_{ac} . The temperature and frequency window of the χ_{ac} experiments were not ample enough to inform about the maxima of the $g(D)$ distributions, instead upper bounds for these maxima are shown in the table. Due to the assumption of a functional form, this difficulty does not exist when using the $M(H)$ data, although, for the same reason, the so determined $g(D)$ maximum must be considered with a limited confidence.

At this stage, we should also indicate that, although it is informative, the localization of the maxima of the distributions (see Table II) is *dependent* on the chosen representation [either $g(D)$ or $f(D)$]. On the contrary, the distributions

themselves *do actually contain* the complete information about the cluster sizes determined by both methods.

Although the structure of the zeolite lattice and hence the dimensions and geometry of their pores and cavities is known, there is no *direct* evidence of the actual size of the clusters. It is very likely the existence of clusters with very particular geometries, for example, clusters occupying two or three contiguous supercages, magnetically correlated by exchange interaction through the intercage pores.¹¹ This possibility is a natural explanation for the presence of particles greater than about 13 Å. This criticism can also be extended to understand previous experiments on sample Z1S, which suggested a bimodal distribution of cluster sizes.²⁶ Finally we observe that the results obtained by means of both magnetic methods for Z1S and Z2 are congruous with the particle size upper limit determined by TEM. The sample Z1B, as has previously been explained, may possess some damage in the cavity structure in such a way that Z3, the sample actually observed by TEM, may not be representative enough.

To further characterize the experimental $f(D)$ data resulting from the ac susceptibility scaling (shown in Fig. 7) we have tried to fit them to a log-normal function. This test cannot be applied to sample Z2 because it lacks enough points at low diameters (left side in the figure). Data corresponding to Z1B do not behave in a log-normal manner, due obviously to the presence of a small shoulder at the right-hand side of the distribution. Finally, a satisfactory log-normal fit was also impossible to achieve with the Z1S data.

VI. CONCLUSIONS

In this work, the magnetic behavior of a dilute assembly of magnetic clusters in a crystalline matrix is presented. The paper mainly focused on the determination of the size distribution of the clusters from magnetic data. Particularly, the characterization of systems like zeolites, or inhomogeneous materials obtained from thermal treatments, needs granulometric methods able to give account of *any* kind of distribution without imposing *a priori* its functional form.

The ac susceptibility, because of its dynamic character, has been evidenced as a useful tool in distinguishing between relaxational and static effects as would occur, respectively, between single-particle superparamagnetic blocking and phase transitions due to dipole-dipole interaction. The analysis of the frequency and temperature dependence of the ac susceptibility appears to be a valuable method in obtaining the distribution of activation energies.

Although the conversion from activation energies to par-

ticle sizes is subjected to practical difficulties, the $f(D)$ distribution obtained from the scaling of χ_{ac} supplies information otherwise invisible from standard analysis of the magnetization curve. In particular, samples Z1S and Z2 are good examples of systems with narrow distributions and full absence of particles above a certain diameter. Besides, in general, the method that assumes a log-normal distribution seems not to be an adequate description of these cluster assemblies.

The meaning of the ac susceptibility scaling plot is related to the traditional fit of the susceptibility peak temperatures at different frequencies [Eq. (4)], but has the advantage of covering the whole distribution of activation energies, only lim-

ited by the frequency and the temperature window of the experiment.

ACKNOWLEDGMENTS

This work has been financed by Diputación General de Aragón (DGA) under Project No. PIT0892, Fundación Domingo Martínez, CICYT Project No. MAT 92-0896-C02-02, and the Deutsche Forschungsgemeinschaft under Project No. TR97/13-3. We are grateful to A. X. Trautwein for many fruitful discussions and his support of this work. One of us, J.L.G., thanks DGA for a grant (BIT 1292).

-
- ¹J. C. Mallinson, *The Foundations of Magnetic Recording* (Academic, New York, 1987).
- ²S. W. Charles and J. Popplewell, *Ferromagnetic Liquids*, edited by E. P. Wohlfarth, Ferromagnetic Materials Vol. 2 (North-Holland, Amsterdam, 1980).
- ³P. V. Hendriksen, S. Linderorth, and P. A. Lindgård, *Phys. Rev. B* **48**, 7259 (1993).
- ⁴M. P. Morales, C. Pecharromán, T. González Carreño, and C. J. Serna, *J. Solid State Chem.* **108**, 158 (1994).
- ⁵J. P. Bucher, D. C. Douglass, and L. A. Bloomfield, *Phys. Rev. Lett.* **66**, 3052 (1991).
- ⁶R. Sessoli, D. Gatteschi, A. Caneschi, and M. A. Novak, *Nature* **365**, 141 (1993).
- ⁷M. El-Hilo, K. O'Grady, and R. W. Chantrell, *J. Magn. Magn. Mater.* **114**, 295 (1992).
- ⁸J. L. Dormann, L. Bessais, and D. Fiorani, *J. Phys. C* **21**, 2015 (1988).
- ⁹R. F. Ziolo, E. P. Giannelis, B. A. Weinstein, M. P. O'Horo, B. N. Ganguly, V. Mehrotra, M. W. Russell, and D. R. Huffman, *Science* **257**, 219 (1992).
- ¹⁰D. W. Breck, *Zeolite Molecular Sieves* (Wiley, New York, 1974).
- ¹¹Y. Nozue, T. Kodaira, and T. Goto, *Phys. Rev. Lett.* **68**, 3789 (1992).
- ¹²V. Schünemann, H. Winkler, Ch. Butzlaff, and A. X. Trautwein, *Hyperfine Interact.* **93**, 1427 (1994).
- ¹³V. Alfredsson, O. Terasaki, and J.-O. Bovin, *J. Solid State Chem.* **105**, 223 (1993).
- ¹⁴A. Meagher, V. Nair, and R. Szostak, *Zeolites* **8**, 3 (1988).
- ¹⁵J. L. García, F. J. Lázaro, C. Martínez, and A. Corma, *J. Magn. Magn. Mater.* **140-144**, 363 (1995).
- ¹⁶H. D. Williams, K. O'Grady, M. El-Hilo, R. W. Chantrell, *J. Magn. Magn. Mater.* **122**, 129 (1993), and references therein.
- ¹⁷R. W. Chantrell, J. Popplewell, and S. W. Charles, *IEEE Trans. Mag.* **14**, 975 (1978).
- ¹⁸C. Djega-Mariadassou and J. L. Dormann, in *Magnetic Properties of Fine Particles*, edited by J. L. Dormann and D. Fiorani (Elsevier, Amsterdam, 1992), p. 191.
- ¹⁹M. El-Hilo, K. O'Grady, and R. W. Chantrell, *J. Magn. Magn. Mater.* **117**, 21 (1992).
- ²⁰E. P. Wohlfarth, *Phys. Lett.* **70A**, 489 (1979).
- ²¹J. I. Gittleman, B. Abeles, and S. Bozowski, *Phys. Rev. B* **9**, 3891 (1974).
- ²²L. Lundgren, P. Svedlindh, and O. Beckman, *J. Magn. Magn. Mater.* **25**, 33 (1981).
- ²³F. J. Lázaro, J. L. García, V. Schünemann, and A. X. Trautwein, *IEEE Trans. Mag.* **29**, 2652 (1993).
- ²⁴S. B. Slade, L. Gunther, F. T. Parker, and A. E. Berkowitz, *J. Magn. Magn. Mater.* **140-144**, 661 (1995).
- ²⁵F. Bødker, S. Mørup, and S. Linderorth, *Phys. Rev. Lett.* **72**, 282 (1994).
- ²⁶V. Schünemann, H. Winkler, H. M. Ziethen, A. Schiller, and A. X. Trautwein, in *Magnetic Properties of Fine Particles*, edited by J. L. Dormann and D. Fiorani (Elsevier, Amsterdam, 1992), p. 371.
- ²⁷In fact, the quantity obtained from FMR is the anisotropy field H_K . This anisotropy constant was calculated by assuming $K = \frac{1}{2}H_K M_s$, M_s being the saturation magnetization of α -Fe.